

This discussion paper is/has been under review for the journal Atmospheric Chemistry and Physics (ACP). Please refer to the corresponding final paper in ACP if available.

Discussion Paper | Discussion Paper

Discussion Paper | Discussion Paper | Discussion Paper | Discussion Paper

Discussion Paper | Discussion Paper | Discussion Paper | Discussion Paper | Discussion Paper

Chemistry of new particle growth in mixed urban and biogenic emissions – insights from CARES

A. Setyan^{1,*}, C. Song², M. Merkel³, W. B. Knighton⁴, T. B. Onasch⁵,
M. R. Canagaratna⁵, D. R. Worsnop^{5,6}, A. Wiedensohler³, J. E. Shilling², and
Q. Zhang¹

¹Department of Environmental Toxicology, 1 Shields Ave., University of California, Davis, CA 95616, USA

²Atmospheric Sciences and Global Change Division, Pacific Northwest National Laboratory, Richmond, WA 99352, USA

³Leibniz Institute for Tropospheric Research, 04318 Leipzig, Germany

⁴Montana State University, Bozeman, MT 59717, USA

⁵Aerodyne Research Inc., Billerica, MA 01821, USA

⁶Department of Physics, University of Helsinki, 00014 Helsinki, Finland

* now at: Département Sciences de l'Atmosphère et Génie de l'Environnement, Ecole Nationale Supérieure des Mines de Douai, 59508 Douai Cedex, France

2043

Received: 29 December 2013 – Accepted: 12 January 2014 – Published: 23 January 2014

Correspondence to: Q. Zhang (dkwzhang@ucdavis.edu)

Published by Copernicus Publications on behalf of the European Geosciences Union.

2044

Abstract

Regional new particle formation and growth events (NPE) were observed on most days over the Sacramento and western Sierra Foothills area of California in June 2010 during the Carbonaceous Aerosols and Radiative Effect Study (CARES). Simultaneous particle measurements at both the T0 (Sacramento, urban site) and the T1 (Cool, rural site located \sim 40 km northeast of Sacramento) sites of CARES indicate that the NPE usually occurred in the morning with the appearance of an ultrafine mode centered at \sim 15 nm (in mobility diameter, D_m , measured by a scanning mobility particle sizer operating in the range 10–858 nm) followed by the growth of this mode to \sim 50 nm in the afternoon. These events were generally associated with southwesterly winds bringing urban plumes from Sacramento to the T1 site. The growth rate was on average higher at T0 ($7.1 \pm 2.7 \text{ nm h}^{-1}$) than at T1 ($6.2 \pm 2.5 \text{ nm h}^{-1}$), likely due to stronger anthropogenic influences at T0. Using a high-resolution time-of-flight aerosol mass spectrometer (HR-ToF-AMS), we investigated the evolution of the size-resolved chemical composition of new particles at T1. Our results indicate that the growth of new particles was driven primarily by the condensation of oxygenated organic species and, to a lesser extent, ammonium sulfate. New particles appear to be fully neutralized during growth, consistent with high NH_3 concentration in the region. Nitrogen-containing organic ions (i.e., CHN^+ , CH_4N^+ , $\text{C}_2\text{H}_3\text{N}^+$, and $\text{C}_2\text{H}_4\text{N}^+$) that are indicative of the presence of alkyl-amine species in submicrometer particles enhanced significantly during the NPE days, suggesting that amines might have played a role in these events. Our results also indicate that the bulk composition of the ultrafine mode organics during NPE was very similar to that of anthropogenically-influenced secondary organic aerosol (SOA) observed in transported urban plumes. In addition, the concentrations of species representative of urban emissions (e.g., black carbon, CO, NO_x , and toluene) were significantly higher whereas the photo-oxidation products of biogenic VOC and the biogenically-influenced SOA also increased moderately during the NPE days compared to the non-event days. These results indicate that the frequently occurring NPE over the Sacramento and

2045

Sierra Nevada regions were mainly driven by urban plumes from Sacramento and that the interaction of regional biogenic emissions with the urban plumes has enhanced the new particle growth. This finding has important implication for quantifying the climate impacts of NPE on global scale.

1 Introduction

New particle formation and growth processes are an important source of ultrafine particles in both clean and polluted environments. A large number of studies reported the observations of intensive new particle events at various locations, including urban areas (e.g., Brock et al., 2003; Dunn et al., 2004; Stanier et al., 2004; Zhang et al., 2004; Wu et al., 2007; Ahlm et al., 2012), remote sites (e.g., Weber et al., 1999; Creamean et al., 2011; Vakkari et al., 2011; Pikridas et al., 2012), forested locations (e.g., Allan et al., 2006; Pierce et al., 2012; Han et al., 2013), coastal sites (e.g., O'Dowd et al., 2002; Wen et al., 2006; Liu et al., 2008; Modini et al., 2009), and polar regions (e.g., Komppula et al., 2003; Koponen et al., 2003; Asmi et al., 2010). These events significantly affect the number concentrations and size distributions of particles in the atmosphere with important implications on human health and climate (Spracklen et al., 2006; Bzdek and Johnston, 2010; Kermanen et al., 2012). However, despite frequent observations, the chemical processes underlying the formation and growth of new particles remain poorly understood.

New particle events occur in two steps, i.e., the formation of nuclei, followed by the growth of the stable clusters to larger sizes by condensation of low-volatility compounds and coagulation. For ambient measurements, the evolution of the number-based particle size distribution is a main criterion for identifying the onset of new particle events. Scanning mobility particle sizer (SMPS), also called mobility particle size spectrometer (MPSS), is the most widely used instrument to determine the particle number concentration and size distribution during these events. The evolution of the chemical composition of ultrafine particles during new particle formation and growth is another

2046

piece of critical information needed for understanding this process. For that purpose, aerosol mass spectrometer (AMS) (e.g., Zhang et al., 2004; Allan et al., 2006; Ziembka et al., 2010; Creamean et al., 2011; Ahlm et al., 2012), chemical ionization mass spectrometer (CIMS) (e.g., Dunn et al., 2004; Smith et al., 2005, 2008, 2010; Jokinen et al., 2012), Nano aerosol mass spectrometer (NAMS) (e.g., Bzdek et al., 2011, 2012), and atmospheric pressure ionization time-of-flight (APi-TOF) mass spectrometer (Lehtipalo et al., 2011; Kulmala et al., 2013) have been successfully deployed in the field to study the chemical processes underlying atmospheric new particle events.

An important finding from previous studies is that organics and sulfates are usually involved in the growth of new particles up to sizes where they can act as cloud condensation nuclei (CCN). The contribution of these two species to particle growth depends on the concentrations of the precursors and meteorological conditions. For example, at urban or industrial locations where the SO_2 mixing ratio is high, sulfate is an important contributor to the growth of new particles (Brock et al., 2003; Zhang et al., 2004; Yue et al., 2010; Bzdek et al., 2012). At rural and remote locations, however, the growth of new particles was found to be almost exclusively driven by organics (Smith et al., 2008; Laaksonen et al., 2008; Ziembka et al., 2010; Pierce et al., 2012; Ahlm et al., 2012). In addition, it was found that in Pittsburgh, USA, despite high ambient SO_2 concentrations, H_2SO_4 contributes mainly to the early stage of the new particle growth, while the growth up to CCN sizes is mainly driven by secondary organic aerosols (SOA), especially during late morning and afternoon when photochemistry is more intense (Zhang et al., 2004, 2005).

SOA is a major component of fine particles globally (Zhang et al., 2007; Jimenez et al., 2009). Understanding its roles in new particle formation and growth is important for addressing aerosols' effects on climate and human health. Recent studies found significantly enhanced SOA formation rates in mixed biogenic and anthropogenic emissions (de Gouw et al., 2005; Volkamer et al., 2006; Kleinman et al., 2008; Setyan et al., 2012; Shilling et al., 2013). However, there is little known about the influence of the interactions of organic species from biogenic and anthropogenic sources on new particle

2047

growth. The Sacramento Valley in California is a place of choice to study this process. The Sacramento metropolitan area lies in the Central Valley to the north of the San Joaquin River Delta and to the southwest of the forested Sierra Nevada Mountains. The wind in this region is characterized by a very regular pattern, especially in summer (Fast et al., 2012). Indeed, during the day, a southwesterly wind usually brings air masses from the San Francisco Bay to the Sacramento metropolitan area and pushes northeast to the Sierra Nevada Mountains (Dillon et al., 2002), promoting the transport of urban plumes from Sacramento to forested regions where biogenic emissions are intense.

The US Department of Energy (DOE) sponsored Carbonaceous Aerosols and Radiative Effects Study (CARES) that took place in the Sacramento Valley in June 2010 was designed to take advantage of this regular wind pattern to better understand the life-cycle processes and radiative properties of carbonaceous aerosols in a region influenced by both anthropogenic and biogenic emissions (Zaveri et al., 2012). Within the framework of CARES, a wide range of instruments were deployed between 2 and 28 June 2010 at two ground sites located in Sacramento (T0, urban site) and Cool, CA at the foothills of the Sierra Nevada Mountains (T1, rural site), respectively, to measure size-resolved chemical compositions, number size distributions, and optical and hygroscopic properties of aerosols, as well as trace gases and meteorological data (Zaveri et al., 2012). One of the major observations during CARES was that particles were dominated by organics in this region, and that the formation of SOA was enhanced when anthropogenic emissions from the Sacramento metropolitan area and the Bay Area were transported to the foothills and mixed with biogenic emissions (Setyan et al., 2012; Shilling et al., 2013).

During CARES, new particle growth events were observed almost daily at both the T0 and T1 sites. Similarly, previous studies conducted at the University of California Blodgett Forest Research Station, approximately 75 km to the northeast of Sacramento and 35 km to the northeast of the T1 site, also reported the frequent occurrence of NPE (Lunden et al., 2006; Creamean et al., 2011). In their study conducted from May

2048

to September 2002, Lunden et al. (2006) found that the oxidation products of reactive biogenic compounds accounted for a significant portion of the particle growth. The study of Creamean et al. (2011), which took place in early spring of 2009, found that sulfates and amines participated in the growth of new particles and that long-range transport of SO_2 from Asia seemed to contribute to faster growth. These findings indicate that new particle formation and growth are important processes in Northern California and are affected by regional anthropogenic and biogenic emissions as well as by pollutants transported from Asia. Understanding how these emissions may govern the NPE's requires measurements of size-resolved chemical compositions of the new particles. The main aim of the present paper is to examine the evolution characteristics of new particles at the T0 and T1 sites during CARES, with a focus on the evolution of size-resolved particle chemical composition based on HR-ToF-AMS measurements at T1.

2 Experimental

2.1 Sampling site and instrumentation

The T0 sampling site was located on the campus of the American River College in Sacramento ($38^{\circ}39'01''$ N, $121^{\circ}20'49''$ W, 30 m a.s.l.) and the T1 site was located on the campus of the Northside School at Cool ($38^{\circ}52'16''$ N, $121^{\circ}01'22''$ W, 450 m a.s.l.). Sacramento is the capital of California, with 480 000 inhabitants in the city and 2.5 million people living in the metropolitan area. Cool is a small town (2500 inhabitants) surrounded by very large forested areas, and located \sim 40 km northeast of Sacramento at the Sierra Nevada foothills.

Size-resolved chemical composition of non-refractory submicron aerosols (NR- PM_1) were measured using an Aerodyne HR-AMS (DeCarlo et al., 2006; Canagaratna et al., 2007). A detailed discussion on its operation at T1 during the present study was presented in Setyan et al. (2012). Briefly, the HR-AMS was equipped with an aerodynamic

2049

lens allowing the transmission of particles in the range \sim 30–1500 nm (in vacuum aerodynamic diameter, D_{va}). The instrument was operated alternatively in V- and W-mode every 2.5 min. In V-mode, data was recorded in mass spectrum (MS) mode and particle time-of-flight (PToF) mode. The MS mode was used to obtain average mass spectra and determine the concentration of the species in submicrometer particles without size information. In the PToF mode, average mass spectra were acquired for 92 size bins covering 30–1500 nm (D_{va}), allowing the determination of the size-resolved chemical composition. W-mode data was recorded exclusively in MS mode.

The particle number size distribution was measured with a SMPS (also called MPSS, type TROPOS) as described in Wiedensohler et al. (2012). The instrument used at T1 consists of a Hauke-type differential mobility analyzer (DMA) and a condensation particle counter (CPC; TSI Inc., Shoreview, MN; model 3772), and used ^{210}Po as radioactive source for the neutralizer (Setyan et al., 2012). The SMPS was set to measure particles in the range 10–858 nm (in mobility diameter, D_{m}), divided into 70 logarithmically distributed size bins. SMPS data has been corrected to take into account the DMA-CPC lag time, bipolar charge distribution, CPC efficiency, and diffusion loss. The SMPS deployed at T0 was a commercial instrument (TSI Inc.; model 3936), and was constituted of a ^{85}Kr neutralizer, a DMA (TSI Inc.; model 3080 with the long column) and a CPC (TSI Inc.; model 3775). The instrument measured particles in the size range of 12–737 nm (in D_{m}) divided into 115 size bins. Diffusion loss correction was applied after the data inversion. All dates and times reported in this paper are in Pacific Daylight Time (PDT = UTC – 7 h), which was the local time during this study.

2.2 Data analysis

Particle number concentration and size distribution have been used to identify new particle events in the atmosphere. However, given that the new particles formed by nucleation have generally a diameter in the size range 1–3 nm, smaller than the smallest size measured by our SMPS's, we were not able to observe the new particle formation themselves during the present study, but only the growth of the newly formed particles

2050

that are larger than 10 nm. For this reason, we will not use the terms “nucleation” or “new particle formation” in the forthcoming discussion, but rather “new particle growth”. Each day for which complete SMPS data was available was classified as new particle event (NPE) day if the particle number concentration in the size range 12–20 nm increased by more than 800 particles cm^{-3} , and if this increase was accompanied by the increase of the mode during the following hours. These two conditions allowed us to distinguish NPE from primary emissions from vehicles, which also produce small particles but are usually observed as occasional spikes in the time series of the particle number concentration in the range 12–20 nm. In addition, each growth event was considered as “strong” if the increase of the particle number concentration in the range 12–20 nm was higher than 1500 particles cm^{-3} , and “weak” if the increase was lower than this threshold. A summary of the new particle growth events observed during this study is provided in Table 1.

The mode(s) of each particle number size distribution recorded during this study have been determined with a multiple peak fitting tool available in Igor Pro 6.2.2.2 (WaveMetrics Inc., Lake Oswego, OR). The growth rate (GR), which corresponds to the increase of the mode of newly formed particles per time unit (nm h^{-1}), has been calculated for each individual growth event using Eq. (1):

$$\text{GR} = \frac{\Delta D_m}{\Delta t} \quad (1)$$

in which ΔD_m is the difference of the mode (nm) between the beginning of the growth and the period when the growth significantly slows down, and Δt is the duration of the growth (h).

2051

3 Results and discussions

3.1 Evolution of particle number size distributions during regional new particle events

The SMPSs were fully operational during 26 days at T0, and 22 days at T1, from 2–29 June 2010. The time series of the particle number size distributions show that new particle events frequently occurred at both sites (Fig. 1), indicating that these events occurred on a regional scale. A total of 19 NPE were identified at T1 (86 % of the time; Table 1), eight of which were considered as “strong” and eleven as “weak”. Most of the events (14 in total) occurred during periods of southwesterly wind that transported urban plumes to the T1 site (i.e., T0 → T1), except for 5 events which occurred during northwesterly wind periods (Table 1). In addition, all 8 strong NPE occurred during the T0 → T1 periods (Table 1). At T0, 22 new particle events were identified, 18 of which were considered as “strong” and only four events were “weak”.

Generally, the increase of the particle number concentration during these events was higher at T0 than at T1 (average 9.6E3 vs. 3.8E3 # $\text{cm}^{-3} \text{h}^{-1}$; Table 1) and the average ($\pm 1\sigma$) growth rate of new particles was slightly higher at T0 ($7.1 \pm 2.7 \text{ nm h}^{-1}$ vs. $6.2 \pm 2.5 \text{ nm h}^{-1}$ at T1). The occurrence of relatively stronger and faster NPE at T0 is likely due to the proximity of emission sources of precursor species and a higher anthropogenic influence. Indeed, the frequency as well as the growth rates observed during the present study were much higher than those reported by Lunden et al. (2006) at ~35 km northeast of T1 (frequency = 30 % of the time, average growth rate = $3.8 \pm 1.9 \text{ nm h}^{-1}$), where the lower frequency and growth rates might be related to the fact that their site was located deeper into the forest and subjected to relatively lesser anthropogenic influences from urban areas to the southwest (e.g., Sacramento and the San Francisco Bay Area). The growth rates measured during the present study are also much higher than those observed at Hytiälä, Finland, where NPE have been extensively observed and described over the past 15 yr. Riipinen et al. (2011) report a median growth rate of 2.3 nm h^{-1} during the years 2003–2007, much lower than at

2052

Cool (6.2 nm h^{-1}) and Sacramento (7.1 nm h^{-1}). NPE at Hyttiälä are mainly driven by the photooxidation of biogenic precursors. The Sacramento and Sierra Foothill region, however, is influenced by both urban and biogenic emission sources. Thus, the comparison between the growth rates at these different sites suggests that the degree of anthropogenic influence may be an important factor driving the growth rate.

During the present study, all growth events began in the morning, with the appearance of a nucleation mode observed with the SMPS between 09:00 and 12:00 (PDT). Particle growth lasted several hours, with size modes reaching their maximum in the afternoon, typically after 15:00. The modes at the end of the growth in general peaked between 40–50 nm, but for several cases, the mode did not reach 35 nm, especially for the weakest events or when a change in the wind direction was observed during the day (Fig. 1).

An important observation of the present study is that NPE began at T1 a few hours later than at T0, especially during days characterized with daytime T0 → T1 transport. A typical example of this phenomenon occurred on 26 June (Figs. 2 and 3). According to Fast et al. (2012), a T0 to T1 transport occurred that day. Particles smaller than 20 nm (in D_m) began to increase slightly before 09:00 at T0 (Fig. 2a), and a nucleation mode appeared at the same time (Fig. 3). Then, during the following hours, the mode increased slowly up to $\sim 50 \text{ nm}$ (in D_m), likely due to agglomeration and condensation of low-volatility compounds onto the surface of these new particles. Thus, as shown in Fig. 2a, the evolution of the particle number size distribution shows a “banana shape”, which is a typical observation with the SMPS for the growth of new particles. At T1, the same phenomenon occurred at $\sim 11:00$, i.e., 2 h after T0 (Fig. 2b). This time delay is consistent with the wind data recorded at T1 which indicate the sampling of air masses transported from the T0 direction. Further evidence for this pseudo Lagrangian sampling is the observation of a sudden change in wind direction at $\sim 14:30$ at T0 that brought in a very clean air mass associated with a sharp decrease of particle number concentration that lasted for $\sim 3.5 \text{ h}$ (Fig. 2a). Particle concentration at T0 increased again at $\sim 18:00$ after a shift of the wind direction back to southwesterly. A mirrored

2053

decrease of particle concentration, although less dramatically, was observed at 16:30 at T1, $\sim 2 \text{ h}$ after the clean air mass event at T0 (Fig. 2b). The increase of particle number concentration occurred at T1 around 21:00, $\sim 3 \text{ h}$ after the increase occurred at T1, consistent with gradually decreasing wind speed from 16:30 to 21:00. The wind direction at T1 remained southwesterly during the entire afternoon (Fig. 2b).

This time delay between T0 and T1 was also observed during the other events, and this is confirmed by the diurnal evolution profiles of the size distributions at both sites (Fig. 4a and c). These observations indicate that new particle growth generally occurred during T0 → T1 transport promoted by the daytime southwesterly wind and that the new particle growth events were generally more intense at T0 compared to at T1. Wind rose plot during NPE (Fig. 5g) confirms that these events usually occurred when the wind was coming from the southwest, which corresponds to the location of the Sacramento metropolitan area. On the other hand, when NPE was not observed, the wind was coming mainly from the northwest and the west (Fig. 5h), bringing air masses dominated by biogenic emissions (Setyan et al., 2012), thus reducing anthropogenic influences at T1.

It is interesting to notice that the evolution of the particle number size distributions and concentrations during the evening and the night is not similar at T0 and T1. At T0, particle number concentration remains almost constant between 23:00 and 08:00, while the mode is centered at $\sim 35\text{--}40 \text{ nm}$ (in D_m) during this period (Fig. 4a). On the contrary, particle number concentration decreases gradually at T1 during night, while the mode increases from 35 nm (at 21:00) up to 90 nm (at 14:00 the following day; Fig. 4c). This may be due to the fact that the T0 site was more influenced by nanoparticles from vehicular emissions than the T1 site, due to the proximity of traffic, anthropogenic emissions, and transport from the Bay Area. On the other hand, the T1 site was more influenced by downslope winds during the night, when a change in the wind direction brought down more aged aerosols from the Sierra Nevada to the foothills (Setyan et al., 2012).

2054

3.2 Evolution of particle chemistry during new particle growth

The evolution of particle chemistry during NPE at T1 was studied in detail with a HR-ToF-AMS. As summarized in Table 1, the increase of particle number concentration during the new particle growth events was accompanied by an increase of organics and sulfate in ultrafine particles (40–120 nm in D_{va}). The average ($\pm 1\sigma$) increase of organics in that size range was 0.71 (± 0.29) $\mu\text{g m}^{-3}$ while that of sulfate was 0.10 (± 0.11) $\mu\text{g m}^{-3}$.

Figure 5 shows the diurnal size distributions of organic matter, sulfate, and particle volume concentrations, along with the wind rose plots during NPE days and non-event days. The growth of new particles was mainly contributed by sulfate and organics (Fig. 5a and c), but the increase of particle mass observed by the AMS occurred after 11:00, later than the increase of number concentration according to the SMPS. This is because the smallest size measured by our SMPS is 10 nm (in D_m), while the transmission through the AMS is significant only for particles larger than 30 nm (in D_{va}) (Jayne et al., 2000). Given that particle density at T1 was on average 1.4 during this study (Setyan et al., 2012), and assuming that they are spherical, the smallest particles measured by the AMS correspond to ~ 21 nm in D_m . Thus, the SMPS was the first instrument to detect the growth of new particles, while the HR-ToF-AMS observed the growth 2 or 3 h later, depending on the growth rate. A similar observation was reported during NPE in Pittsburgh (Zhang et al., 2004). It is interesting to notice that organics, sulfate, and particle volume exhibit qualitatively the same diurnal size distributions (Fig. 5). Indeed, they have a constant mode in larger particles during the entire day, and they increase in ultrafine particles in the afternoon during the growth events.

The diurnal patterns of organics and sulfate in three different size ranges (40–120, 120–200, and 200–800 nm in D_{va}) show that their afternoon increase occurred mainly in ultrafine particles (40–120 nm) while the increases in the rest of the sizes were moderate during NPE days (Fig. 6a and c). In comparison, the diurnal profiles of both species were relatively flat and their concentrations much lower during the non-event

2055

days (Fig. 6b and d). Although both organics and sulfate in ultrafine particles increased in the afternoon, the increase of the organic mass in the 40–120 nm particles was on average 7 times higher than that of sulfate (see above and Fig. 7d and e). Clearly, the growth of new particles was mainly driven by organics. This is in agreement with previous studies, which also emphasized the key-role of organics in the growth of new particles up to CCN sizes (Smith et al., 2008; Laaksonen et al., 2008; Ziembka et al., 2010; Zhang et al., 2011; Pierce et al., 2012; Ahlm et al., 2012; Riipinen et al., 2012).

Another important observation is the substantial increase of the signals of four nitrogen-containing ions (i.e., CHN^+ , CH_4N^+ , $\text{C}_2\text{H}_3\text{N}^+$, and $\text{C}_2\text{H}_4\text{N}^+$) in submicron particles during the new particle growth periods (Fig. 7f). On average, the concentration of these ions during NPE days was 2.4 times the concentration observed during non-NPE days (Fig. 10). Since these $\text{C}_x\text{H}_y\text{N}^+$ ions are generally related to alkyl-amine species (Ge et al., 2014), this class of compounds was likely involved in the growth of new particles. This is consistent with previous findings in the atmosphere (e.g., Makela et al., 2001; Smith et al., 2008, 2010; Bzdek et al., 2011; Creamean et al., 2011; Laitinen et al., 2011). Recent studies have found that sulfuric acid–amine clusters are highly stable and that even trace amount of amines (e.g., a few ppt) can enhance particle formation rates by orders of magnitude compared with ammonia (Almeida et al., 2013; Zollner et al., 2012). The importance of gas-phase amines in the generation of organic salts involved in the formation of new particles was also confirmed by thermodynamic modeling study (Barsanti et al., 2009). Based on the mass spectrometry fragmentation patterns of amine standards analyzed in our lab (Ge et al., 2014), the average concentration of aminium ($\text{R}_1\text{R}_2\text{R}_3\text{N}^+$, where R_1 , R_2 , R_3 are either H or an alkyl group) is estimated to be approximately 1/10th that of ammonium at T1 during this study (Fig. 7f). Although we are unable to directly assess the importance of amines in new particle formation based on this study, our results suggest that amines likely played an important role in the formation of new particles in the Sacramento and Sierra foothills region.

2056

Due to the high contribution of organics to submicron aerosol mass in the region, positive matrix factorization (PMF) analysis was performed on the high resolution mass spectra of the AMS to investigate the sources and processes of organic aerosols (Setyan et al., 2012). Briefly, three distinct factors were determined, including a biogenically-influenced SOA associated with the regional biogenic emissions (O/C ratio = 0.54, 40 % of total organic mass), an anthropogenically-influenced SOA associated with transported urban plumes (O/C ratio = 0.42, 51 %), and a hydrocarbon-like organic aerosol (HOA) mainly associated with local primary emissions (O/C ratio = 0.08, 9 %). Details on the determination and validation of these three OA types are given in Setyan et al. (2012). It is important to clarify here that the biogenic SOA and urban transport SOA identified at T1 do not correspond to SOAs formed from 100 % anthropogenic or biogenic precursors. In fact, the so-called biogenic SOA was found in air masses with dominant biogenic influence and little anthropogenic influence, while the urban transport SOA was found in air masses characterized as urban plumes mixed with the continuously present biogenic emissions in the region. These observations are consistent with radiocarbon analysis of fine particulate matter, which has shown that modern carbon worldwide often contributes > 70 % of the total carbon, particularly downwind of urban areas (Glasius et al., 2011; Schichtel et al., 2008 and references therein).

As shown in Fig. 7, during NPE days, the mass concentration of urban transport SOA increased by more than a factor of 2 (from 0.75 to $1.7 \mu\text{g m}^{-3}$) between 10:00 and 16:00 (Fig. 7b), whereas that of biogenic SOA increased only slightly by ~ 10 % during that period (from $0.84\text{--}0.93 \mu\text{g m}^{-3}$, Fig. 7c). This result underlines the key-role played by the urban plumes from Sacramento in the NPE events at Sierra foothills.

Figure 8 shows the evolutions of the mass-weighted size distributions of Org, SO_4^{2-} , organic tracer ions, and particle number distributions during daytime. The average size distributions of Org and SO_4^{2-} during NPE days show significant increase of concentrations in the small mode (Fig. 8e and g). On the other hand, the increases of the

2057

concentrations of Org and SO_4^{2-} in ultrafine particles were all negligible during non-event days (Fig. 8f and h).

Another important parameter to determine was the neutralization of sulfate in the ultrafine mode during NPE. We already know from the mass spectral mode of the AMS that sulfate was fully neutralized in the bulk during the entire study (Setyan et al., 2012). Many previous studies mentioned that sulfate involved in NPE was usually under the form of sulfuric acid, especially during the initial steps of the growth (Brock et al., 2003; Zhang et al., 2004; Yue et al., 2010; Bzdek et al., 2012). However, northern California contains very large agricultural regions with a lot of sources of ammonia, which could possibly neutralize sulfate in the ultrafine mode. Using high mass resolution mass spectra acquired under PToF mode, we determined the size distributions of ammonium and sulfate based on those of the NH_3^+ and SO^+ , which are the ions of ammonium and sulfate, respectively, with the highest signal-to-noise ratio (see Supplement for details of this data treatment). As shown in Fig. 9, despite relatively noisy data, the size distributions suggest that sulfate was fully neutralized by ammonium in the entire size range, including ultrafine particles. Moreover, we did not observe any difference in the sulfate neutralization between NPE and non-NPE days or between different times of the day. These results indicate that sulfate in ultrafine particles was present in the form of ammonium sulfate and that sulfuric acid was quickly neutralized after condensation.

3.3 Anthropogenic influence on new particle growth events

The average concentrations and diurnal patterns of VOCs, trace gases (O_3 , CO, NO_x), BC, and meteorological parameters (temperature, relative humidity, and solar radiation) during NPE days and non-event days were compared (Figs. 10, S3 and S4, and Table 2). An important difference between NPE and non-event days was the concentrations of photo-oxidation products (formaldehyde and acetaldehyde) and anthropogenic precursors (BC, CO and toluene), which were all significantly higher during NPE days than during non-event days. Photo-oxidation products were on average ~ 50 %

2058

more concentrated on NPE days (formaldehyde: 2.71 ± 1.39 ppb vs. 1.83 ± 0.81 ppb during non-NPE days; acetaldehyde: 0.97 ± 0.47 ppb vs. 0.71 ± 0.24 ppb). The sum of methacrolein (MACR) and methyl vinyl ketone (MVK), which are the first generational products of isoprene oxidation, was also $\sim 20\%$ higher during NPE days: 5 0.98 ± 0.79 ppb vs. 0.75 ± 0.50 ppb. These results suggest that the condensation of these compounds, and likely other compounds co-generated during photo-oxidation, onto the surface of particles could be an important factor driving the growth of new particles. Moreover, the diurnal patterns of these compounds during NPE and non-NPE 10 days show a clear difference during the afternoon, whereas these differences are much smaller during nighttime (Fig. S4). This result stresses the influence of photochemistry on the formation and growth of new particles.

The average concentrations of isoprene were almost identical during NPE and non-event days (Fig. 10). Comparatively, the enhancements of anthropogenic species during NPE days were more dramatic. The average concentrations of BC ($0.042 \pm 15 0.028 \mu\text{g m}^{-3}$ during NPE days vs. $0.027 \pm 0.017 \mu\text{g m}^{-3}$ during non-NPE days), CO (130 ± 27.0 vs. 99.8 ± 19.8 ppb), NO_x (3.8 ± 3.3 vs. 2.7 ± 3.5 ppb), HOA (0.16 ± 0.15 vs. $0.11 \pm 0.08 \mu\text{g m}^{-3}$), and toluene (0.060 ± 0.037 vs. 0.038 ± 0.019 ppb; Table 2) were significantly ($30\text{--}60\%$) higher on NPE days. The ozone concentrations, however, were very similar between two types of days (46.2 ± 10.5 ppb during non-NPE 20 vs. 43.5 ± 14.2 ppb). These results point out the importance of the anthropogenic influence on the formation and growth of new particles, most of these events occurring in the urban plume from Sacramento. However, during a study undertaken at the Blodgett Forest, which is located ~ 35 km on the northeast of the present sampling site and ~ 75 km downwind from Sacramento, Lunden et al. (2006) observed new particle 25 growth events when the degree of anthropogenic influence was significantly reduced.

It is interesting to note that the relative humidity (RH) was on average 18% higher on NPE days ($45 \pm 13\%$) compared to non-event days ($27 \pm 12\%$). Previous studies, however, found contradictory links between new particle growth events and RH. For example, Lunden et al. (2006) and Charron et al. (2007) observed growth events when

2059

RH was high, while non-event days were characterized by significantly lower RH. In addition, most of the previous studies reported NPE when the RH was low (Boy and Kulmala, 2002; Hamed et al., 2007, 2011; Jeong et al., 2010; Guo et al., 2012). The exact role of RH in new particle formation and growth is not clearly elucidated yet. 5 According to Hamed et al. (2011), who used a combination of field data, theoretical calculations and numerical models, the anti-correlation between RH and new particle growth would simply be due to the fact that solar radiation and photochemistry usually peak at noon when the RH exhibits its lower value. However, this does not seem to have influenced the growth events of the present study, since the weather was sunny 10 during the entire field campaign. The only point is that the RH was much lower during northwesterly wind periods (Setyan et al., 2012), during which we usually did not observe growth events.

Figure 11 shows the average size-resolved mass spectra of organics in $40\text{--}120$ nm (D_{va}) particles during NPE days and non-event days, along with the mass spectra of 15 biogenic SOA and urban transport SOA reported in Setyan et al. (2012). The average mass spectrum of organics before the growth (i.e., between 08:00 and 10:00) was subtracted in order to remove the influence of particles existing before the start of the growth events. Therefore, the spectra shown in Fig. 11 are the average mass spectra of organic matter that contributed to the growth of $40\text{--}120$ nm particles between 10:00–16:00 during NPE days ($\Delta\text{Org}_{40\text{--}120\text{ nm}}^{\text{NPE}}$) and during non-event days ($\Delta\text{Org}_{40\text{--}120\text{ nm}}^{\text{non-NPE}}$), 20 respectively. As shown in Fig. 11a, the spectrum of $\Delta\text{Org}_{40\text{--}120\text{ nm}}^{\text{NPE}}$ is dominated by the signal at m/z 44 (mostly CO_2^+), while that of m/z 43 (mostly $\text{C}_2\text{H}_3\text{O}^+$) is approximately the half of it. The spectrum of $\Delta\text{Org}_{40\text{--}120\text{ nm}}^{\text{NPE}}$ is very similar to that of urban transport SOA ($r^2 = 0.95$; Fig. 11b) but its correlation coefficient towards the spectrum 25 of biogenic SOA is lower ($r^2 = 0.87$). On the other hand, the spectrum of $\Delta\text{Org}_{40\text{--}120\text{ nm}}^{\text{non-NPE}}$ is very similar to that of biogenic SOA, as shown by the scatterplot of Fig. 11d. We further performed multilinear regression analyses to represent the mass spectra of $\Delta\text{Org}_{40\text{--}120\text{ nm}}^{\text{NPE}}$ and $\Delta\text{Org}_{40\text{--}120\text{ nm}}^{\text{non-NPE}}$, respectively, as the linear combinations of the spectra of urban transport SOA and biogenic SOA. Based on this analysis, we estimated

2060

that during NPE days, ~74 % of the organic mass that contributed to the growth of ultrafine particles was SOA formed in urban transport plumes. During non-event days, the growth of ultrafine mode organics, which was much slower compared during NPE, was primarily (~76 % by mass) due to SOA influenced by regional biogenic emissions.

These results, coupled to the higher concentrations of anthropogenic compounds on NPE days suggest that the growth of new particles in the Sierra Nevada Foothills was mainly driven by anthropogenic precursors transported from Sacramento and that the growth was likely promoted by the interaction between urban plumes and biogenic emissions. These observations may have important implications in our understanding of SOA formation. For example, models used to assess global SOA budget tend to underpredict the SOA concentrations. However, in a recent study, Spracklen et al. (2011) used a model to estimate the global OA source, and compared their results with worldwide AMS observations. When they took into account anthropogenically-controlled biogenic SOA formation in their estimation of the global OA budget, it reduced considerably the bias between their model and AMS observations.

4 Conclusions

New particle growth events were frequently observed during the US DOE's CARES campaign in northern California in June 2010. Presented here is a description of these events observed with two SMPSs deployed at Sacramento (T0, urban site) and Cool (T1, rural site at the Sierra foothills). Our results showed that these growth events took place on a regional scale, predominantly during periods of southwestern flow that transports urban plumes and anthropogenic emissions from the Sacramento metropolitan area and the San Francisco Bay Area near Carquinez Strait. Growth rates were on average higher at T0 ($7.1 \pm 2.7 \text{ nm h}^{-1}$) than at T1 ($6.2 \pm 2.5 \text{ nm h}^{-1}$), likely due to higher anthropogenic influences at T0. The evolution of the size-resolved chemical composition of these newly formed particles has been investigated in detail with a HR-ToF-AMS deployed at T1. Our results indicate that the new particle growth was mainly

2061

driven by organics, with a small contribution of ammonium sulfate. For example, the average increase of the organic mass in ultrafine particles (40–120 nm in D_{va} , which corresponds to 30–85 nm in Stokes (volume equivalent) diameter, assuming no internal voids, sphericity = 1, and density = 1.4 g cm^{-3}) was $0.7 \mu\text{g m}^{-3}$ during this period, approximately 7 times higher than that of sulfate ($0.1 \mu\text{g m}^{-3}$). Our results also indicate that amines were enhanced significantly during the new particle growth, suggesting that this class of compounds likely played a role. The size-resolved mass spectra of organics in the size range 40–120 nm (in D_{va}) during the growth events were very similar to the mass spectrum of anthropogenically-influenced SOA from urban plume. In addition, during the NPE days, the concentrations of photo-oxidation products (formaldehyde, acetaldehyde, sum of methacrolein and methyl vinyl ketone) and species representative of urban emissions (e.g., BC, CO, NO_x , HOA, and toluene) were on average 50 % higher than during non-event days. These results suggest that the new particle growth events were mainly driven by the transported urban plumes and that the growth of new particles was enhanced by the interactions between biogenic emissions and transported urban plumes.

**Supplementary material related to this article is available online at
[http://www.atmos-chem-phys-discuss.net/14/2043/2014/
acpd-14-2043-2014-supplement.pdf](http://www.atmos-chem-phys-discuss.net/14/2043/2014/acpd-14-2043-2014-supplement.pdf).**

Acknowledgements. This research was supported by the US Department of Energy (DOE), the Office of Science (BER), Atmospheric System Research Program, grant No. DE-FG02-11 ER65293, the California Air Resources Board (CARB), Agreement No. 10-305, and the California Agricultural Experiment Station, Project CA-DETX-2102-H.

2062

References

Ahlm, L., Liu, S., Day, D. A., Russell, L. M., Weber, R., Gentner, D. R., Goldstein, A. H., Di Gangi, J. P., Henry, S. B., Keutsch, F. N., VandenBoer, T. C., Markovic, M. Z., Murphy, J. G., Ren, X., and Scheller, S.: Formation and growth of ultrafine particles from secondary sources in bakersfield, california, *J. Geophys. Res.*, 117, D00V08, doi:10.1029/2011jd017144, 2012.

Allan, J. D., Alfarra, M. R., Bower, K. N., Coe, H., Jayne, J. T., Worsnop, D. R., Aalto, P. P., Kulmala, M., Hytöläinen, T., Cavalli, F., and Laaksonen, A.: Size and composition measurements of background aerosol and new particle growth in a Finnish forest during QUEST 2 using an Aerodyne Aerosol Mass Spectrometer, *Atmos. Chem. Phys.*, 6, 315–327, doi:10.5194/acp-6-315-2006, 2006.

Almeida, J., Schobesberger, S., Kurten, A., Ortega, I. K., Kupiainen-Maatta, O., Praplan, A. P., Adamov, A., Amorim, A., Bianchi, F., Breitenlechner, M., David, A., Dommen, J., Donahue, N. M., Downard, A., Dunne, E., Duplissy, J., Ehrhart, S., Flagan, R. C., Franchin, A., Guida, R., Hakala, J., Hansel, A., Heinritzi, M., Henschel, H., Jokinen, T., Junninen, H., Kajos, M., Kangasluoma, J., Keskinen, H., Kupc, A., Kurten, T., Kvashin, A. N., Laaksonen, A., Lehtipalo, K., Leiminger, M., Leppa, J., Loukonen, V., Makhmutov, V., Mathot, S., McGrath, M. J., Nieminen, T., Olenius, T., Onnela, A., Petaja, T., Riccobono, F., Riipinen, I., Rissanen, M., Rondo, L., Ruuskanen, T., Santos, F. D., Sarnela, N., Schallhart, S., Schnitzhofer, R., Seinfeld, J. H., Simon, M., Sipila, M., Stozhkov, Y., Stratmann, F., Tome, A., Trostl, J., Tsagkogeorgas, G., Vaattovaara, P., Viisanen, Y., Virtanen, A., Vrtala, A., Wagner, P. E., Weingartner, E., Wex, H., Williamson, C., Wimmer, D., Ye, P. L., Yli-Juuti, T., Carslaw, K. S., Kulmala, M., Curtius, J., Baltensperger, U., Worsnop, D. R., Vehkamaki, H., and Kirkby, J.: Molecular understanding of sulphuric acid-amine particle nucleation in the atmosphere, *Nature*, 502, 359–363, doi:10.1038/nature12663, 2013.

Asmi, E., Frey, A., Virkkula, A., Ehn, M., Manninen, H. E., Timonen, H., Tolonen-Kivimäki, O., Aurela, M., Hillamo, R., and Kulmala, M.: Hygroscopicity and chemical composition of Antarctic sub-micrometre aerosol particles and observations of new particle formation, *Atmos. Chem. Phys.*, 10, 4253–4271, doi:10.5194/acp-10-4253-2010, 2010.

Barsanti, K. C., McMurry, P. H., and Smith, J. N.: The potential contribution of organic salts to new particle growth, *Atmos. Chem. Phys.*, 9, 2949–2957, doi:10.5194/acp-9-2949-2009, 2009.

2063

Boy, M. and Kulmala, M.: Nucleation events in the continental boundary layer: Influence of physical and meteorological parameters, *Atmos. Chem. Phys.*, 2, 1–16, doi:10.5194/acp-2-1-2002, 2002.

Brock, C. A., Trainer, M., Ryerson, T. B., Neuman, J. A., Parrish, D. D., Holloway, J. S., Nicks Jr., D. K., Frost, G. J., Hübner, G., Fehsenfeld, F. C., Wilson, J. C., Reeves, J. M., Lafleur, B. G., Hilbert, H., Atlas, E. L., Donnelly, S. G., Schaufler, S. M., Stroud, V. R., and Wiedinmyer, C.: Particle growth in urban and industrial plumes in Texas, *J. Geophys. Res.*, 108, 4111, doi:10.1029/2002jd002746, 2003.

Bzdek, B. R. and Johnston, M. V.: New particle formation and growth in the troposphere, *Anal. Chem.*, 82, 7871–7878, doi:10.1021/ac100856j, 2010.

Bzdek, B. R., Zordan, C. A., Luther, G. W., and Johnston, M. V.: Nanoparticle chemical composition during new particle formation, *Aerosol Sci. Tech.*, 45, 1041–1048, doi:10.1080/02786826.2011.580392, 2011.

Bzdek, B. R., Zordan, C. A., Pennington, M. R., Luther, G. W., and Johnston, M. V.: Quantitative assessment of the sulfuric acid contribution to new particle growth, *Environ. Sci. Technol.*, 46, 4365–4373, doi:10.1021/es204556c, 2012.

Canagaratna, M. R., Jayne, J. T., Jimenez, J. L., Allan, J. D., Alfarra, M. R., Zhang, Q., Onasch, T. B., Drewnick, F., Coe, H., Middlebrook, A., Delia, A., Williams, L. R., Trimborn, A. M., Northway, M. J., DeCarlo, P. F., Kolb, C. E., Davidovits, P., and Worsnop, D. R.: Chemical and microphysical characterization of ambient aerosols with the aerodyne aerosol mass spectrometer, *Mass Spectrom. Rev.*, 26, 185–222, doi:10.1002/mas.20115, 2007.

Charron, A., Birmili, W., and Harrison, R. M.: Factors influencing new particle formation at the rural site, harwell, United Kingdom, *J. Geophys. Res.*, 112, D14210, doi:10.1029/2007jd008425, 2007.

Creamean, J. M., Ault, A. P., Ten Hoeve, J. E., Jacobson, M. Z., Roberts, G. C., and Prather, K. A.: Measurements of aerosol chemistry during new particle formation events at a remote rural mountain site, *Environ. Sci. Technol.*, 45, 8208–8216, doi:10.1021/es103692f, 2011.

de Gouw, J. A., Middlebrook, A. M., Warneke, C., Goldan, P. D., Kuster, W. C., Roberts, J. M., Fehsenfeld, F. C., Worsnop, D. R., Canagaratna, M. R., Pszenny, A. A. P., Keene, W. C., Marchewka, M., Bertman, S. B., and Bates, T. S.: Budget of organic carbon in a polluted atmosphere: results from the new england air quality study in 2002, *J. Geophys. Res.-Atmos.*, 110, D16305, doi:10.1029/2004jd005623, 2005.

2064

DeCarlo, P. F., Kimmel, J. R., Trimborn, A., Northway, M. J., Jayne, J. T., Aiken, A. C., Gonin, M., Fuhrer, K., Horvath, T., Docherty, K. S., Worsnop, D. R., and Jimenez, J. L.: Field-deployable, high-resolution, time-of-flight aerosol mass spectrometer, *Anal. Chem.*, **78**, 8281–8289, doi:10.1021/ac061249n, 2006.

5 Dillon, M. B., Lamanna, M. S., Schade, G. W., Goldstein, A. H., and Cohen, R. C.: Chemical evolution of the sacramento urban plume: transport and oxidation, *J. Geophys. Res.-Atmos.*, **107**, 4045, doi:10.1029/2001jd000969, 2002.

Dunn, M. J., Jiménez, J.-L., Baumgardner, D., Castro, T., McMurry, P. H., and Smith, J. N.: Measurements of mexico city nanoparticle size distributions: observations of new particle formation and growth, *Geophys. Res. Lett.*, **31**, L10102, doi:10.1029/2004gl019483, 2004.

10 Fast, J. D., Gustafson Jr., W. I., Berg, L. K., Shaw, W. J., Pekour, M., Shrivastava, M., Barnard, J. C., Ferrare, R. A., Hostetler, C. A., Hair, J. A., Erickson, M., Jobson, B. T., Flowers, B., Dubey, M. K., Springston, S., Pierce, R. B., Dolislager, L., Pederson, J., and Zaveri, R. A.: Transport and mixing patterns over Central California during the carbonaceous aerosol and radiative effects study (CARES), *Atmos. Chem. Phys.*, **12**, 1759–1783, doi:10.5194/acp-12-1759-2012, 2012.

Glasius, M., la Cour, A., and Lohse, C.: Fossil and nonfossil carbon in fine particulate matter: A study of five european cities, *J. Geophys. Res.-Atmos.*, **116**, D11302, doi:10.1029/2011jd015646, 2011.

20 Guo, H., Wang, D. W., Cheung, K., Ling, Z. H., Chan, C. K., and Yao, X. H.: Observation of aerosol size distribution and new particle formation at a mountain site in subtropical Hong Kong, *Atmos. Chem. Phys.*, **12**, 9923–9939, doi:10.5194/acp-12-9923-2012, 2012.

Hamed, A., Joutsensaari, J., Mikkonen, S., Sogacheva, L., Dal Maso, M., Kulmala, M., Cavalli, F., Fuzzi, S., Facchini, M. C., Decesari, S., Mircea, M., Lehtinen, K. E. J., and Laaksonen, A.: Nucleation and growth of new particles in Po Valley, Italy, *Atmos. Chem. Phys.*, **7**, 355–376, doi:10.5194/acp-7-355-2007, 2007.

25 Hamed, A., Korhonen, H., Sihto, S. L., Joutsensaari, J., Jarvinen, H., Petaja, T., Arnold, F., Nieminen, T., Kulmala, M., Smith, J. N., Lehtinen, K. E. J., and Laaksonen, A.: The role of relative humidity in continental new particle formation, *J. Geophys. Res.-Atmos.*, **116**, D03202, doi:10.1029/2010jd014186, 2011.

30 Han, Y., Iwamoto, Y., Nakayama, T., Kawamura, K., Hussein, T., and Mochida, M.: Observation of new particle formation over a mid-latitude forest facing the north pacific, *Atmos. Environ.*, **64**, 77–84, doi:10.1016/j.atmosenv.2012.09.036, 2013.

2065

Jayne, J. T., Leard, D. C., Zhang, X. F., Davidovits, P., Smith, K. A., Kolb, C. E., and Worsnop, D. R.: Development of an aerosol mass spectrometer for size and composition analysis of submicron particles, *Aerosol Sci. Tech.*, **33**, 49–70, doi:10.1080/027868200410840, 2000.

5 Jeong, C.-H., Evans, G. J., McGuire, M. L., Chang, R. Y.-W., Abbatt, J. P. D., Zeromskiene, K., Mozurkewich, M., Li, S.-M., and Leaitch, W. R.: Particle formation and growth at five rural and urban sites, *Atmos. Chem. Phys.*, **10**, 7979–7995, doi:10.5194/acp-10-7979-2010, 2010.

Jimenez, J. L., Canagaratna, M. R., Donahue, N. M., Prevot, A. S. H., Zhang, Q., Kroll, J. H., DeCarlo, P. F., Allan, J. D., Coe, H., Ng, N. L., Aiken, A. C., Docherty, K. S., Ulbrich, I. M., Grieshop, A. P., Robinson, A. L., Duplissy, J., Smith, J. D., Wilson, K. R., Lanz, V. A., Hueglin, C., Sun, Y. L., Tian, J., Laaksonen, A., Raatikainen, T., Rautiainen, J., Vaattovaara, P., Ehn, M., Kulmala, M., Tomlinson, J. M., Collins, D. R., Cubison, M. J., Dunlea, E. J., Huffman, J. A., Onasch, T. B., Alfarra, M. R., Williams, P. I., Bower, K., Kondo, Y., Schneider, J., Drewnick, F., Borrmann, S., Weimer, S., Demerjian, K., Salcedo, D., Cottrell, L., Griffin, R., Takami, A., Miyoshi, T., Hatakeyama, S., Shimono, A., Sun, J. Y., Zhang, Y. M., Dzepina, K., Kimmel, J. R., Sueper, D., Jayne, J. T., Herndon, S. C., Trimborn, A. M., Williams, L. R., Wood, E. C., Middlebrook, A. M., Kolb, C. E., Baltensperger, U., and Worsnop, D. R.: Evolution of organic aerosols in the atmosphere, *Science*, **326**, 1525–1529, doi:10.1126/science.1180353, 2009.

10 Jokinen, T., Sipilä, M., Junninen, H., Ehn, M., Lönn, G., Hakala, J., Petäjä, T., Mauldin III, R. L., Kulmala, M., and Worsnop, D. R.: Atmospheric sulphuric acid and neutral cluster measurements using CI-API-TOF, *Atmos. Chem. Phys.*, **12**, 4117–4125, doi:10.5194/acp-12-4117-2012, 2012.

Kerminen, V.-M., Paramonov, M., Anttila, T., Riipinen, I., Fountoukis, C., Korhonen, H., Asmi, E., 15 Laakso, L., Lihavainen, H., Swietlicki, E., Svenningsson, B., Asmi, A., Pandis, S. N., Kulmala, M., and Petäjä, T.: Cloud condensation nuclei production associated with atmospheric nucleation: a synthesis based on existing literature and new results, *Atmos. Chem. Phys.*, **12**, 12037–12059, doi:10.5194/acp-12-12037-2012, 2012.

Kleinman, L. I., Springston, S. R., Daum, P. H., Lee, Y.-N., Nunnermacker, L. J., Senum, G. I., 20 Wang, J., Weinstein-Lloyd, J., Alexander, M. L., Hubbe, J., Ortega, J., Canagaratna, M. R., and Jayne, J.: The time evolution of aerosol composition over the Mexico City plateau, *Atmos. Chem. Phys.*, **8**, 1559–1575, doi:10.5194/acp-8-1559-2008, 2008.

2066

Komppula, M., Lihavainen, H., Hatakka, J., Paatero, J., Aalto, P., Kulmala, M., and Viisanen, Y.: Observations of new particle formation and size distributions at two different heights and surroundings in subarctic area in northern finland, *J. Geophys. Res.*, 108, 4295, doi:10.1029/2002jd002939, 2003.

5 Koponen, I. K., Virkkula, A., Hillamo, R., Kerminen, V.-M., and Kulmala, M.: Number size distributions and concentrations of the continental summer aerosols in queen maud land, antarctica, *J. Geophys. Res.*, 108, 4587, doi:10.1029/2003jd003614, 2003.

10 Kulmala, M., Kontkanen, J., Junninen, H., Lehtipalo, K., Manninen, H. E., Nieminen, T., Petäjä, T., Sipilä, M., Schobesberger, S., Rantala, P., Franchin, A., Jokinen, T., Järvinen, E., Äijälä, M., Kangasluoma, J., Hakala, J., Aalto, P. P., Paasonen, P., Mikkilä, J., Vanhanen, J., Aalto, J., Hakola, H., Makkonen, U., Ruuskanen, T., Mauldin, R. L., Duplissy, J., Vehkamäki, H., Bäck, J., Kortelainen, A., Riipinen, I., Kurtén, T., Johnston, M. V., Smith, J. N., Ehn, M., Mentel, T. F., Lehtinen, K. E. J., Laaksonen, A., Kerminen, V.-M., and Worsnop, D. R.: Direct observations of atmospheric aerosol nucleation, *Science*, 339, 943–946, doi:10.1126/science.1227385, 2013.

15 Laaksonen, A., Kulmala, M., O'Dowd, C. D., Joutsensaari, J., Vaattovaara, P., Mikkonen, S., Lehtinen, K. E. J., Sogacheva, L., Dal Maso, M., Aalto, P., Petäjä, T., Sogachev, A., Yoon, Y. J., Lihavainen, H., Nilsson, D., Facchini, M. C., Cavalli, F., Fuzzi, S., Hoffmann, T., Arnold, F., Hanke, M., Sellegrí, K., Umann, B., Junkermann, W., Coe, H., Allan, J. D., Alfarra, M. R., Worsnop, D. R., Riekola, M. -L., Hyötyläinen, T., and Viisanen, Y.: The role of VOC oxidation products in continental new particle formation, *Atmos. Chem. Phys.*, 8, 2657–2665, doi:10.5194/acp-8-2657-2008, 2008.

20 Laitinen, T., Ehn, M., Junninen, H., Ruiz-Jimenez, J., Parshintsev, J., Hartonen, K., Riekola, M. L., Worsnop, D. R., and Kulmala, M.: Characterization of organic compounds in 10-to 50-nm aerosol particles in boreal forest with laser desorption-ionization aerosol mass spectrometer and comparison with other techniques, *Atmos. Environ.*, 45, 3711–3719, doi:10.1016/j.atmosenv.2011.04.023, 2011.

25 Lehtipalo, K., Sipilä, M., Junninen, H., Ehn, M., Berndt, T., Kajos, M. K., Worsnop, D. R., Petäjä, T., and Kulmala, M.: Observations of nano-cn in the nocturnal boreal forest, *Aerosol Sci. Tech.*, 45, 499–509, doi:10.1080/02786826.2010.547537, 2011.

30 Liu, S., Hu, M., Wu, Z., Wehner, B., Wiedensohler, A., and Cheng, Y.: Aerosol number size distribution and new particle formation at a rural/coastal site in pearl river delta (prd) of china, *Atmos. Environ.*, 42, 6275–6283, doi:10.1016/j.atmosenv.2008.01.063, 2008.

2067

Lunden, M. M., Black, D. R., McKay, M., Revzan, K. L., Goldstein, A. H., and Brown, N. J.: Characteristics of fine particle growth events observed above a forested ecosystem in the sierra nevada mountains of california, *Aerosol Sci. Tech.*, 40, 373–388, doi:10.1080/02786820600631896, 2006.

5 Makela, J. M., Yli-Koivisto, S., Hiltunen, V., Seidl, W., Swietlicki, E., Teinila, K., Sillanpaa, M., Koponen, I. K., Paatero, J., Rosman, K., and Hameri, K.: Chemical composition of aerosol during particle formation events in boreal forest, *Tellus B*, 53, 380–393, doi:10.1034/j.1600-0889.2001.530405.x, 2001.

10 Modini, R. L., Ristovski, Z. D., Johnson, G. R., He, C., Surawski, N., Morawska, L., Suni, T., and Kulmala, M.: New particle formation and growth at a remote, sub-tropical coastal location, *Atmos. Chem. Phys.*, 9, 7607–7621, doi:10.5194/acp-9-7607-2009, 2009.

O'Dowd, C. D., Jimenez, J. L., Bahreini, R., Flagan, R. C., Seinfeld, J. H., Hameri, K., Pirjola, L., Kulmala, M., Jennings, S. G., and Hoffmann, T.: Marine aerosol formation from biogenic iodine emissions, *Nature*, 417, 632–636, 2002.

15 Pierce, J. R., Leaitch, W. R., Liggio, J., Westervelt, D. M., Wainwright, C. D., Abbatt, J. P. D., Ahlm, L., Al-Basheer, W., Cziczo, D. J., Hayden, K. L., Lee, A. K. Y., Li, S.-M., Russell, L. M., Sjostedt, S. J., Strawbridge, K. B., Travis, M., Vlasenko, A., Wentzell, J. J. B., Wiebe, H. A., Wong, J. P. S., and Macdonald, A. M.: Nucleation and condensational growth to CCN sizes during a sustained pristine biogenic SOA event in a forested mountain valley, *Atmos. Chem. Phys.*, 12, 3147–3163, doi:10.5194/acp-12-3147-2012, 2012.

20 Pikridas, M., Riipinen, I., Hildebrandt, L., Kostenidou, E., Manninen, H., Mihalopoulos, N., Kalivitis, N., Burkhardt, J. F., Stohl, A., Kulmala, M., and Pandis, S. N.: New particle formation at a remote site in the eastern mediterranean, *J. Geophys. Res.*, 117, D12205, doi:10.1029/2012jd017570, 2012.

25 Riipinen, I., Pierce, J. R., Yli-Juuti, T., Nieminen, T., Häkkinen, S., Ehn, M., Junninen, H., Lehtipalo, K., Petäjä, T., Slowik, J., Chang, R., Shantz, N. C., Abbatt, J., Leaitch, W. R., Kerminen, V.-M., Worsnop, D. R., Pandis, S. N., Donahue, N. M., and Kulmala, M.: Organic condensation: a vital link connecting aerosol formation to cloud condensation nuclei (CCN) concentrations, *Atmos. Chem. Phys.*, 11, 3865–3878, doi:10.5194/acp-11-3865-2011, 2011.

30 Riipinen, I., Yli-Juuti, T., Pierce, J. R., Petaja, T., Worsnop, D. R., Kulmala, M., and Donahue, N. M.: The contribution of organics to atmospheric nanoparticle growth, *Nat. Geosci.*, 5, 453–458, doi:10.1038/ngeo1499, 2012.

2068

Schichtel, B. A., Malm, W. C., Bench, G., Fallon, S., McDade, C. E., Chow, J. C., and Watson, J. G.: Fossil and contemporary fine particulate carbon fractions at 12 rural and urban sites in the united states, *J. Geophys. Res.-Atmos.*, 113, D02311, doi:10.1029/2007jd008605, 2008.

5 Setyan, A., Zhang, Q., Merkel, M., Knighton, W. B., Sun, Y., Song, C., Shilling, J. E., Onasch, T. B., Herndon, S. C., Worsnop, D. R., Fast, J. D., Zaveri, R. A., Berg, L. K., Wiedensohler, A., Flowers, B. A., Dubey, M. K., and Subramanian, R.: Characterization of submicron particles influenced by mixed biogenic and anthropogenic emissions using high-resolution aerosol mass spectrometry: results from CARES, *Atmos. Chem. Phys.*, 12, 8131–8156, doi:10.5194/acp-12-8131-2012, 2012.

10 Shilling, J. E., Zaveri, R. A., Fast, J. D., Kleinman, L., Alexander, M. L., Canagaratna, M. R., Fortner, E., Hubbe, J. M., Jayne, J. T., Sedlacek, A., Setyan, A., Springston, S., Worsnop, D. R., and Zhang, Q.: Enhanced SOA formation from mixed anthropogenic and biogenic emissions during the CARES campaign, *Atmos. Chem. Phys.*, 13, 2091–2113, doi:10.5194/acp-13-2091-2013, 2013.

15 Smith, J. N., Moore, K. F., Eisele, F. L., Voisin, D., Ghimire, A. K., Sakurai, H., and McMurry, P. H.: Chemical composition of atmospheric nanoparticles during nucleation events in atlanta, *J. Geophys. Res.-Atmos.*, 110, D22S03, doi:10.1029/2005jd005912, 2005.

20 Smith, J. N., Dunn, M. J., VanReken, T. M., Iida, K., Stolzenburg, M. R., McMurry, P. H., and Huey, L. G.: Chemical composition of atmospheric nanoparticles formed from nucleation in tecamac, mexico: evidence for an important role for organic species in nanoparticle growth, *Geophys. Res. Lett.*, 35, L04808, doi:10.1029/2007GL032523, 2008.

25 Smith, J. N., Barsanti, K. C., Friedli, H. R., Ehn, M., Kulmala, M., Collins, D. R., Scheckman, J. H., Williams, B. J., and McMurry, P. H.: Observations of aminium salts in atmospheric nanoparticles and possible climatic implications, *P. Natl. Acad. Sci. USA*, 107, 6634–6639, doi:10.1073/pnas.0912127107, 2010.

Spracklen, D. V., Carslaw, K. S., Kulmala, M., Kerminen, V.-M., Mann, G. W., and Sihto, S.-L.: The contribution of boundary layer nucleation events to total particle concentrations on regional and global scales, *Atmos. Chem. Phys.*, 6, 5631–5648, doi:10.5194/acp-6-5631-2006, 2006.

30 Spracklen, D. V., Jimenez, J. L., Carslaw, K. S., Worsnop, D. R., Evans, M. J., Mann, G. W., Zhang, Q., Canagaratna, M. R., Allan, J., Coe, H., McFiggans, G., Rap, A., and Forster, P.:

2069

Aerosol mass spectrometer constraint on the global secondary organic aerosol budget, *Atmos. Chem. Phys.*, 11, 12109–12136, doi:10.5194/acp-11-12109-2011, 2011.

Stanier, C. O., Khlystov, A. Y., and Pandis, S. N.: Nucleation events during the pittsburgh air quality study: description and relation to key meteorological, gas phase, and aerosol parameters, *Aerosol Sci. Tech.*, 38, 253–264, doi:10.1080/02786820390229570, 2004.

5 Vakkari, V., Laakso, H., Kulmala, M., Laaksonen, A., Mabaso, D., Molefe, M., Kgabi, N., and Laakso, L.: New particle formation events in semi-clean South African savannah, *Atmos. Chem. Phys.*, 11, 3333–3346, doi:10.5194/acp-11-3333-2011, 2011.

Volkamer, R., Jimenez, J. L., San Martini, F., Dzepina, K., Zhang, Q., Salcedo, D., Molina, L. T., Worsnop, D. R., and Molina, M. J.: Secondary organic aerosol formation from anthropogenic air pollution: rapid and higher than expected, *Geophys. Res. Lett.*, 33, L17811, doi:10.1029/2006gl026899, 2006.

Weber, R. J., McMurry, P. H., Mauldin, R. L., Tanner, D. J., Eisele, F. L., Clarke, A. D., and Kapturin, V. N.: New particle formation in the remote troposphere: a comparison of observations at various sites, *Geophys. Res. Lett.*, 26, 307–310, doi:10.1029/1998gl900308, 1999.

15 Wen, J., Zhao, Y., and Wexler, A. S.: Marine particle nucleation: observation at bodega bay, california, *J. Geophys. Res.*, 111, D08207, doi:10.1029/2005jd006210, 2006.

Wiedensohler, A., Birmili, W., Nowak, A., Sonntag, A., Weinhold, K., Merkel, M., Wehner, B., Tuch, T., Pfeifer, S., Fiebig, M., Fjäraa, A. M., Asmi, E., Sellegrí, K., Depuy, R., Venzac, H., Villani, P., Laj, P., Aalto, P., Ogren, J. A., Swietlicki, E., Williams, P., Roldin, P., Quincey, P., Hüglin, C., Fierz-Schmidhauser, R., Gysel, M., Weingartner, E., Riccobono, F., Santos, S., Grüning, C., Faloon, K., Beddows, D., Harrison, R., Monahan, C., Jennings, S. G., O'Dowd, C. D., Marinoni, A., Horn, H.-G., Keck, L., Jiang, J., Scheckman, J., McMurry, P. H., Deng, Z., Zhao, C. S., Moerman, M., Henzing, B., de Leeuw, G., Löschau, G., and Bastian, S.: Mobility particle size spectrometers: harmonization of technical standards and data structure to facilitate high quality long-term observations of atmospheric particle number size distributions, *Atmos. Meas. Tech.*, 5, 657–685, doi:10.5194/amt-5-657-2012, 2012.

20 Wu, Z., Hu, M., Liu, S., Wehner, B., Bauer, S., Maßling, A., Wiedensohler, A., Petäjä, T., Dal Maso, M., and Kulmala, M.: New particle formation in beijing, china: statistical analysis of a 1-year data set, *J. Geophys. Res.*, 112, D09209, doi:10.1029/2006jd007406, 2007.

25 Yue, D. L., Hu, M., Zhang, R. Y., Wang, Z. B., Zheng, J., Wu, Z. J., Wiedensohler, A., He, L. Y., Huang, X. F., and Zhu, T.: The roles of sulfuric acid in new particle formation and growth in the

2070

mega-city of Beijing, *Atmos. Chem. Phys.*, 10, 4953–4960, doi:10.5194/acp-10-4953-2010, 2010.

Zaveri, R. A., Shaw, W. J., Cziczo, D. J., Schmid, B., Ferrare, R. A., Alexander, M. L., Alexandrov, M., Alvarez, R. J., Arnott, W. P., Atkinson, D. B., Baidar, S., Banta, R. M., Barnard, J. C., Beranek, J., Berg, L. K., Brechtel, F., Brewer, W. A., Cahill, J. F., Cairns, B., Cappa, C. D., Chand, D., China, S., Comstock, J. M., Dubey, M. K., Easter, R. C., Erickson, M. H., Fast, J. D., Floerchinger, C., Flowers, B. A., Fortner, E., Gaffney, J. S., Gilles, M. K., Gorkowski, K., Gustafson, W. I., Gyawali, M., Hair, J., Hardesty, R. M., Harworth, J. W., Herndon, S., Hiranuma, N., Hostetler, C., Hubbe, J. M., Jayne, J. T., Jeong, H., Jobson, B. T., Kassianov, E. I., Kleinman, L. I., Kluzek, C., Knighton, B., Kolesar, K. R., Kuang, C., Kubátová, A., Langford, A. O., Laskin, A., Laulainen, N., Marchbanks, R. D., Mazzoleni, C., Mei, F., Moffet, R. C., Nelson, D., Oblad, M. D., Oetjen, H., Onasch, T. B., Ortega, I., Ottaviani, M., Pekour, M., Prather, K. A., Radney, J. G., Rogers, R. R., Sandberg, S. P., Sedlacek, A., Senff, C. J., Senum, G., Setyan, A., Shilling, J. E., Shrivastava, M., Song, C., Springston, S. R., Subramanian, R., Suski, K., Tomlinson, J., Volkamer, R., Wallace, H. W., Wang, J., Weickmann, A. M., Worsnop, D. R., Yu, X.-Y., Zelenyuk, A., and Zhang, Q.: Overview of the 2010 Carbonaceous Aerosols and Radiative Effects Study (CARES), *Atmos. Chem. Phys.*, 12, 7647–7687, doi:10.5194/acp-12-7647-2012, 2012.

Zhang, Q., Stanier, C. O., Canagaratna, M. R., Jayne, J. T., Worsnop, D. R., Pandis, S. N., and Jimenez, J. L.: Insights into the chemistry of new particle formation and growth events in pittsburgh based on aerosol mass spectrometry, *Environ. Sci. Technol.*, 38, 4797–4809, doi:10.1021/es035417u, 2004.

Zhang, Q., Worsnop, D. R., Canagaratna, M. R., and Jimenez, J. L.: Hydrocarbon-like and oxygenated organic aerosols in Pittsburgh: insights into sources and processes of organic aerosols, *Atmos. Chem. Phys.*, 5, 3289–3311, doi:10.5194/acp-5-3289-2005, 2005.

Zhang, Q., Jimenez, J. L., Canagaratna, M. R., Allan, J. D., Coe, H., Ulbrich, I., Alfarra, M. R., Takami, A., Middlebrook, A. M., Sun, Y. L., Dzepina, K., Dunlea, E., Docherty, K., DeCarlo, P. F., Salcedo, D., Onasch, T., Jayne, J. T., Miyoshi, T., Shimono, A., Hatakeyama, S., Takegawa, N., Kondo, Y., Schneider, J., Drewnick, F., Borrmann, S., Weimer, S., Demerjian, K., Williams, P., Bower, K., Bahreini, R., Cottrell, L., Griffin, R. J., Rautiainen, J., Sun, J. Y., Zhang, Y. M., and Worsnop, D. R.: Ubiquity and dominance of oxygenated species in organic aerosols in anthropogenically-influenced Northern Hemisphere midlatitudes, *Geophys. Res. Lett.*, 34, L13801, doi:10.1029/2007ql029979, 2007.

2071

Zhang, Y. M., Zhang, X. Y., Sun, J. Y., Lin, W. L., Gong, S. L., Shen, X. J., and Yang, S.: Characterization of new particle and secondary aerosol formation during summertime in beijing, china, Tellus B, 63, 382–394, doi:10.1111/j.1600-0889.2011.00533.x, 2011.

Ziembka, L. D., Griffin, R. J., Cottrell, L. D., Beckman, P. J., Zhang, Q., Varner, R. K., Sive, B. C.,
5 Mao, H., and Talbot, R. W.: Characterization of aerosol associated with enhanced small
particle of number concentrations in a suburban forested environment, *J. Geophys. Res.-*
Atmos., 115, D12206, doi:10.1029/2009jd012614, 2010.

Zollner, J. H., Glasoe, W. A., Panta, B., Carlson, K. K., McMurry, P. H., and Hanson, D. R.:
10 Sulfuric acid nucleation: power dependencies, variation with relative humidity, and effect of
bases, *Atmos. Chem. Phys.*, 12, 4399–4411, doi:10.5194/acp-12-4399-2012, 2012.

2072

Table 1. Summary of the characteristics of new particle growth events observed at Sacramento (T0) and Cool (T1) in northern California.

Day	T0			T1					
	Growth rate nm h ⁻¹	ΔN #cm ⁻³ h ⁻¹	NPE Event	Growth rate nm h ⁻¹	ΔN #cm ⁻³ h ⁻¹	$\Delta \text{Org}_{40-120\text{nm}}$ µg m ⁻³ h ⁻¹	$\Delta \text{SO}_4^{2-}_{40-120\text{nm}}$ µg m ⁻³ h ⁻¹	Wind	NPE Event
2 Jun 2010	Incomplete	SMPS data	N/A ^a	Incomplete	SMPS data	0.75	0.10	T0 → T1 ^b	N/A
3 Jun 2010	10.5	6.12E+03	strong	4.1	2.56E+03	0.98	0.32	T0 → T1	strong
4 Jun 2010	5.4	6.80E+03	strong	12.5	6.14E+03	Incomplete	PtOf data	T0 → T1	strong
5 Jun 2010	10.9	9.57E+03	strong	9.3	1.07E+03	No PtOf data		T0 → T1	weak
6 Jun 2010	12.1	7.40E+03	strong	8.8	2.98E+03	Incomplete	PtOf data	T0 → T1	weak
7 Jun 2010	10.1	6.40E+03	strong	7.6	5.86E+03	0.28	0.063	T0 → T1	strong
8 Jun 2010	4.1	5.64E+03	strong	7.7	4.19E+03	0.35	0.075	T0 → T1	strong
9 Jun 2010	7.3	1.21E+04	strong	6.1	6.92E+03	0.49	0.075	T0 → T1	strong
10 Jun 2010	6.5	7.76E+03	weak	4.2	4.31E+03	0.19	0.0	NW	weak
11 Jun 2010	7.1	2.48E+03	weak	— ^c	—	—	—	NW	no NPG
12 Jun 2010	—	—	no NPG			Incomplete	data	NW	N/A
13 Jun 2010	—	—	no NPG	—	—	—	—	NW	no NPG
14 Jun 2010	4.6	1.26E+04	strong			Incomplete	data	T0 → T1	N/A
15 Jun 2010	4.4	6.75E+03	strong	3.8	4.52E+03	0.27	0.095	T0 → T1	strong
16 Jun 2010	2.5	4.50E+03	strong	3.6	1.59E+03	—	—	NW	weak
17 Jun 2010	—	—	no NPG	2.9	2.28E+03	0.19	0.0	NW	weak
18 Jun 2010	6.7	3.56E+04	strong	4.3	5.30E+03	0.32	0.032	T0 → T1	strong
19 Jun 2010	3.4	2.60E+04	strong	5.9	5.20E+03	0.19	0.041	T0 → T1	weak
20 Jun 2010	4.1	8.69E+03	strong	4.4	2.04E+03	—	—	NW	weak
21 Jun 2010	5.2	4.19E+03	weak	9.5	1.96E+03	0.17	0.0	NW	weak
22 Jun 2010	7.6	1.51E+04	strong			Incomplete	SMPS data	0.10	0.0
23 Jun 2010	11.1	7.28E+03	weak			Incomplete	SMPS data	0.17	0.060
24 Jun 2010	6.4	7.11E+03	strong	7.6	8.28E+03	0.64	0.13	T0 → T1	strong
25 Jun 2010	8.0	4.07E+03	strong	4.7	3.15E+03	0.31	0.0	T0 → T1	weak
26 Jun 2010	7.7	9.13E+03	strong	5.3	1.81E+03	0.27	0.11	T0 → T1	weak
27 Jun 2010	9.3	5.25E+03	strong	5.6	1.34E+03	0.11	0.0	T0 → T1	weak
28 Jun 2010		undefined ^d				—	—	T0 → T1	undefined
mean	7.1	9.57E+03		6.2	3.76E+03	0.34	0.06		
std dev	2.7	7.62E+03		2.5	2.09E+03	0.24	0.08		
median	6.9	7.20E+03		5.6	3.15E+03	0.27	0.06		
min	2.5	2.48E+03		2.9	1.07E+03	0.10	0.0		
max	12.1	3.56E+04		12.5	8.28E+03	0.98	0.32		

^a "N/A" stands for not applicable

^b "T0 → T1" stands for T0 to T1 transport periods

^c “—” means that no increase was observed.

d "undefined" means that the SMPS data did not allow to determine whether a growth event took place or not, because of a change in the wind direction during the day.

2073

Table 2. Summary of average value ± 1 standard deviation for meteorological parameters, particle phase species, and gaseous species during new particle event (NPE) and non-NPE days at the T1 site between 08:00 and 18:00 PDT.

Parameter	NPE days	Non-NPE days
Meteorological data		
Temperature (°C)	24.2 ± 4.4	25.0 ± 4.1
Relative humidity (%)	45.3 ± 12.6	27.1 ± 12.1
Solar radiation (W m ⁻²)	702.9 ± 246.1	792.7 ± 200.4
Particle phase		
Particle number (# cm ⁻³)	9.4E3 ± 6.1E3	4.1E3 ± 1.9E3
Growth rate (nmh ⁻¹)	6.2 ± 2.5	—
Biogenic SOA (μg m ⁻³)	0.90 ± 0.65	0.56 ± 0.27
Urban transport SOA (μg m ⁻³)	1.2 ± 0.90	0.54 ± 0.44
HOA (μg m ⁻³)	0.16 ± 0.15	0.11 ± 0.08
SO ₄ ²⁻ (μg m ⁻³)	0.39 ± 0.22	0.14 ± 0.10
NO ₃ ⁻ (μg m ⁻³)	0.13 ± 0.08	0.054 ± 0.036
BC (μg m ⁻³)	0.042 ± 0.028	0.027 ± 0.017
Trace gases (ppb)		
Terpenes	0.058 ± 0.088	0.043 ± 0.034
Isoprene	1.40 ± 1.02	1.35 ± 0.80
MACR + MVK	0.98 ± 0.79	0.75 ± 0.50
Methanol	6.36 ± 3.12	5.36 ± 1.76
Acetone	1.90 ± 1.09	1.64 ± 0.42
Formaldehyde	2.71 ± 1.39	1.83 ± 0.81
Acetaldehyde	0.97 ± 0.47	0.71 ± 0.24
Acetic acid	0.98 ± 1.10	0.87 ± 0.43
Acetonitrile	0.18 ± 0.03	0.17 ± 0.02
Benzene	0.036 ± 0.029	0.031 ± 0.014
Toluene	0.060 ± 0.037	0.038 ± 0.019
O ₃	43.5 ± 14.2	46.2 ± 10.5
NO _x	3.8 ± 3.3	2.7 ± 3.5
CO	130.1 ± 27.0	99.8 ± 19.8

2074

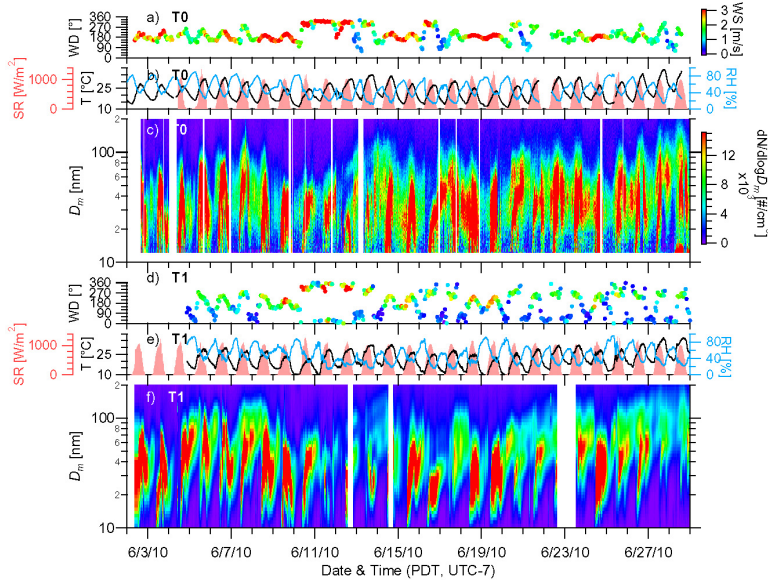


Fig. 1. Time series of (a, d) wind direction colored by wind speed, (b, e) solar radiation, temperature and relative humidity, and (c, f) particle size distributions at the T0 and T1 sites.

2075

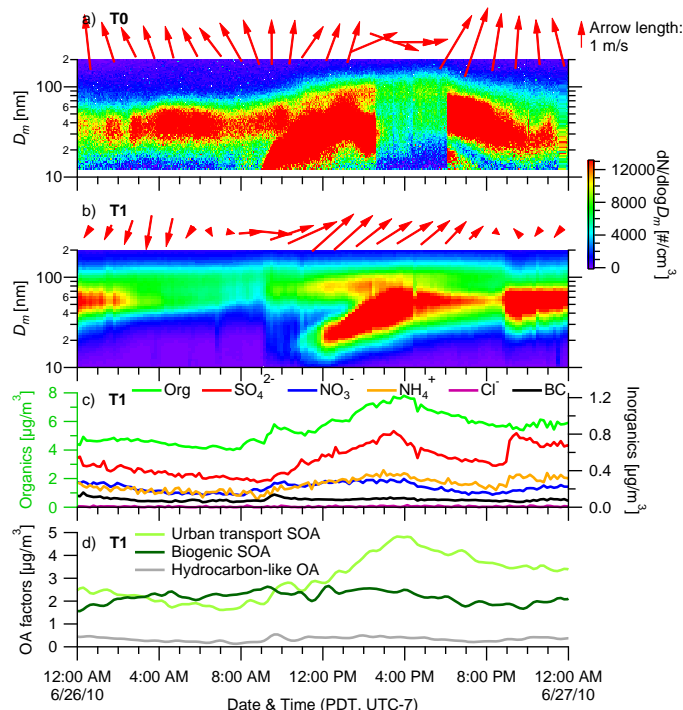


Fig. 2. Comparison of the time evolution of the particle size distributions at the (a) T0 and (b) T1 sites on 26 June, along with the hourly averaged wind direction (length of the arrows is proportional to the wind speed) for each site. Time series of (c) NR-PM₁ species and BC, and (d) three different OA factors.

2076

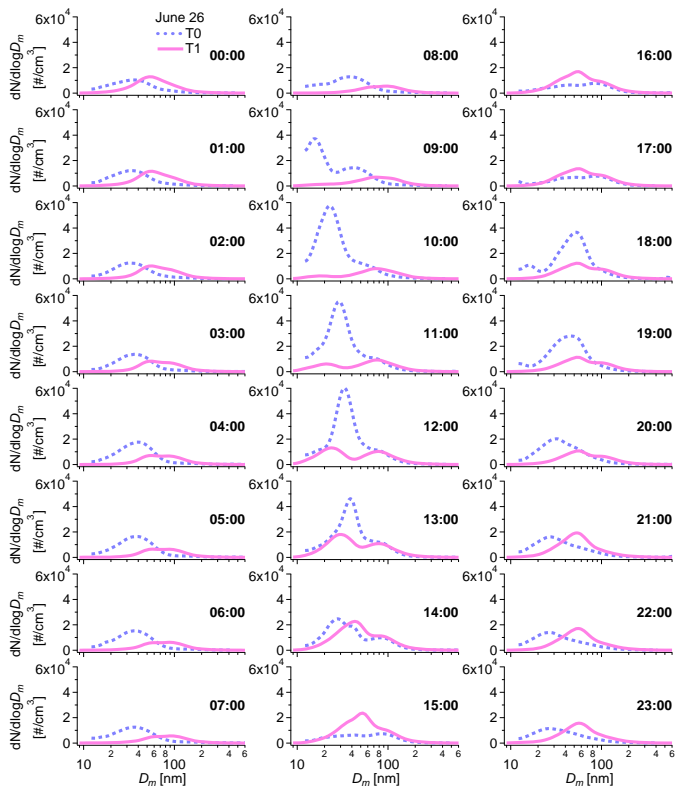


Fig. 3. Comparisons of the average particle number size distributions for each hour at T0 and T1 during 26 June.

2077

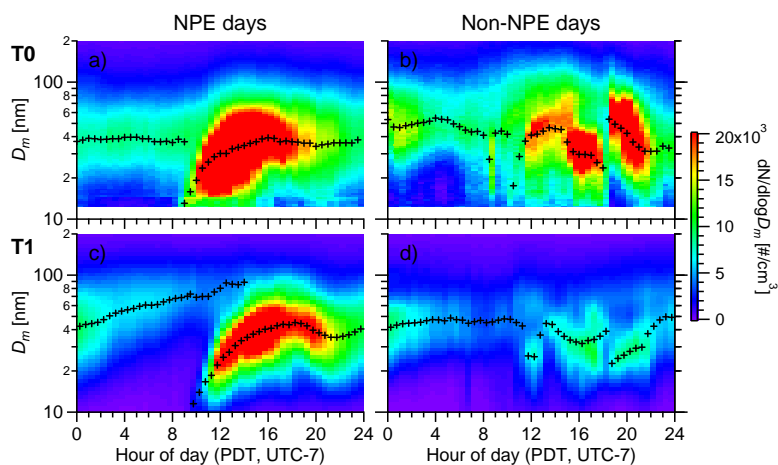


Fig. 4. Diurnal size distributions of the particle number concentration at the (a, b) T0 and (c, d) T1 sites during NPE days (left panel) and non-NPE days (right panel). Black crosses correspond to the modes fitted by log-normal distributions.

2078

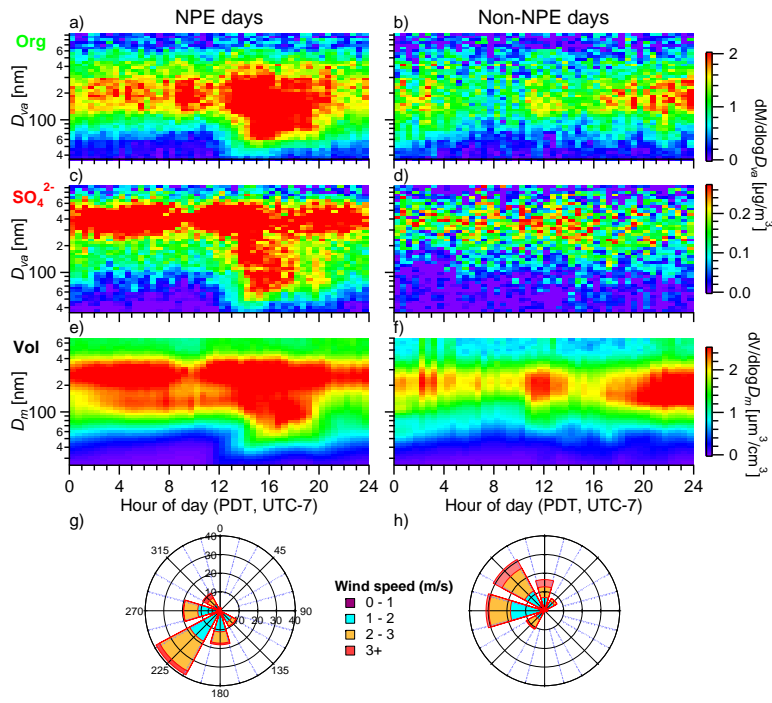


Fig. 5. Diurnal size distributions of (a, b) Org, (c, d) SO_4^{2-} , and (e, f) particle volume concentrations, and (g, h) daytime wind rose plots (08:00–20:00 PDT) for NPE days (left panel) and non-NPE days (right panel).

2079

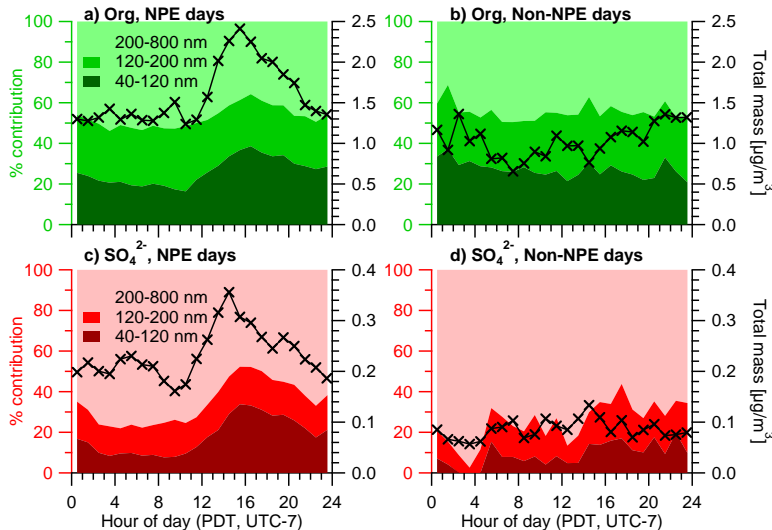


Fig. 6. Diurnal patterns of the concentrations of (a, b) Org and (c, d) SO_4^{2-} and the mass fractions in the range 40–120, 120–200 and 200–800 nm (in D_{va}) during NPE days (left panel) and non-NPE days (right panel).

2080

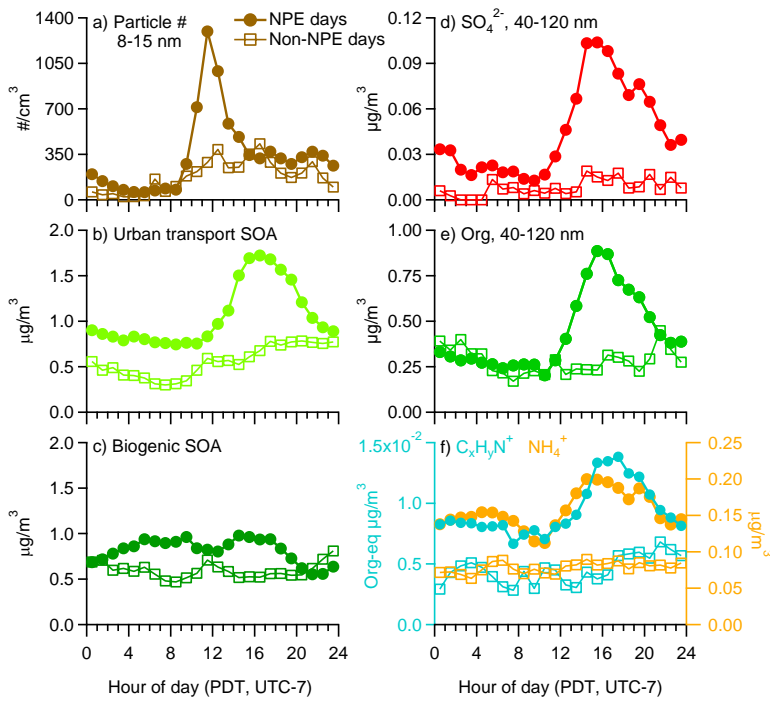


Fig. 7. Diurnal patterns of (a) particle number concentration (10–15 nm), (b) urban transport SOA, (c) biogenic SOA, (d) SO_4^{2-} (40–120 nm in D_{va}), (e) Org (40–120 nm in D_{va}), and (f) N-containing organic ions ($= \text{CHN}^+ + \text{CH}_4\text{N}^+ + \text{C}_2\text{H}_3\text{N}^+ + \text{C}_2\text{H}_4\text{N}^+$) and ammonium during NPE (solid symbols) and non-NPE (open symbols) days.

2081

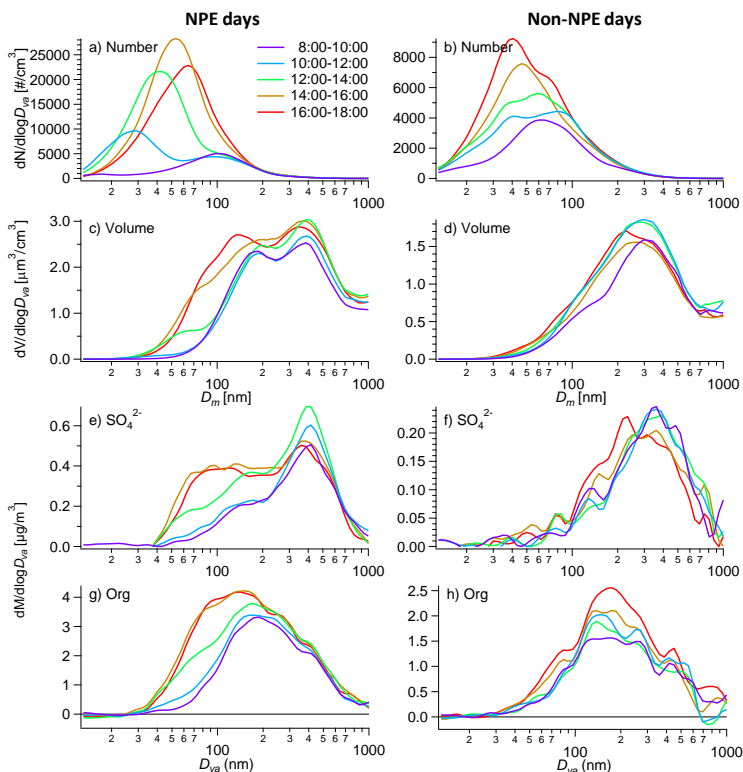


Fig. 8. 2 h averaged size distributions of particle number (a, b) and volume (c, d), SO_4^{2-} (e, f), and Org (g, h) during NPE days (left panel) and non-NPE days (right panel) between 08:00 and 18:00 (PDT).

2082

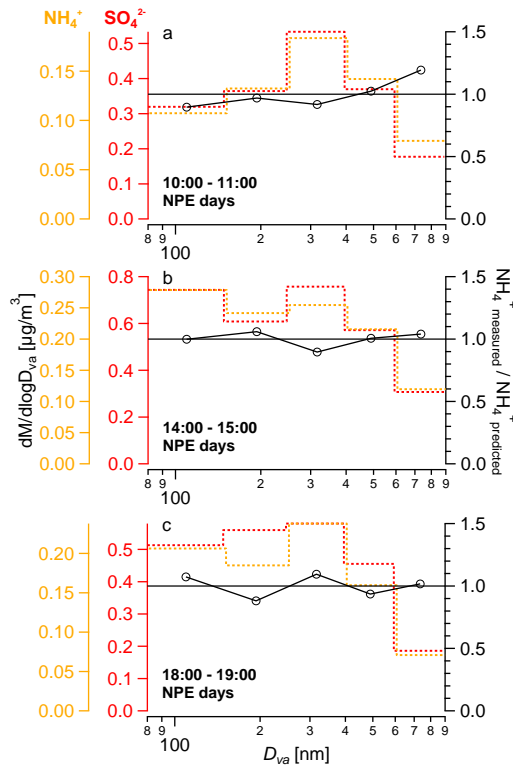


Fig. 9. Size distributions of SO_4^{2-} , NH_4^+ and the ratio of measured NH_4^+ to predicted NH_4^+ ($= \text{SO}_4^{2-} / 48 \times 18$) between 06:00–07:00 (a, b), 10:00–11:00 (c, d), 14:00–15:00 (e, f), and 18:00–19:00 (g, h) during new particle event (NPE; left panels) and non-NPE (right panels) days.

2083

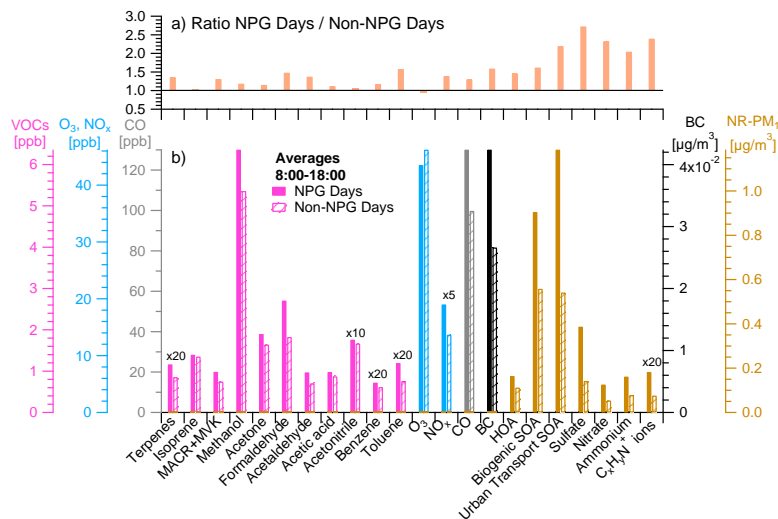


Fig. 10. (b) Average concentrations of VOCs, O_3 , NO_x , CO , BC , NR-PM_1 species, different OA factors, and N-containing organic ions ($= \text{CHN}^+ + \text{CH}_4\text{N}^+ + \text{C}_2\text{H}_3\text{N}^+ + \text{C}_2\text{H}_4\text{N}^+$) between 08:00 and 18:00 (PDT) during NPE and Non-NPE days. (a) NPE days/Non-NPE days ratios for the same parameters.

2084

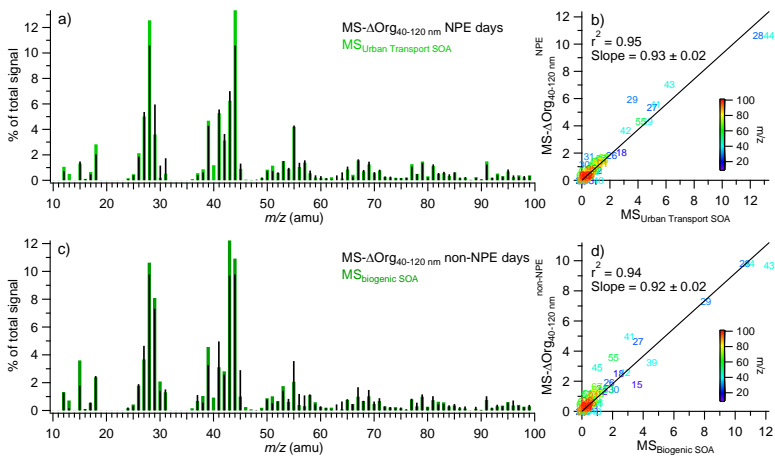


Fig. 11. Average mass spectra of (a) urban transport SOA and Δ Org_{40–120 nm} (i.e., organics that contribute to the growth of 40–120 nm particles) during NPE days, and (c) biogenic SOA and Δ Org_{40–120 nm} during Non-NPE days. Scatterplots that compare the mass spectra of (b) urban transport SOA vs. Δ Org_{40–120 nm} during NPE days, and (d) biogenic SOA vs. Δ Org_{40–120 nm} during non-NPE days.